

Accepted Article

Title: Directing Aluminum Atoms into Energetically Favorable Tetrahedral Sites in Zeolite Framework by Organic Structure-Directing Agents

Authors: Koki Muraoka, Watcharop Chaikittisilp, Yutaka Yanaba, Takeshi Yoshikawa, and Tatsuya Okubo

This manuscript has been accepted after peer review and appears as an Accepted Article online prior to editing, proofing, and formal publication of the final Version of Record (VoR). This work is currently citable by using the Digital Object Identifier (DOI) given below. The VoR will be published online in Early View as soon as possible and may be different to this Accepted Article as a result of editing. Readers should obtain the VoR from the journal website shown below when it is published to ensure accuracy of information. The authors are responsible for the content of this Accepted Article.

To be cited as: *Angew. Chem. Int. Ed.* 10.1002/anie.201713308
Angew. Chem. 10.1002/ange.201713308

Link to VoR: <http://dx.doi.org/10.1002/anie.201713308>
<http://dx.doi.org/10.1002/ange.201713308>

Directing Aluminum Atoms into Energetically Favorable Tetrahedral Sites in Zeolite Framework by Organic Structure-Directing Agents

Koki Muraoka,^[a] Watcharop Chaikittisilp,^{*[a]} Yutaka Yanaba,^[b] Takeshi Yoshikawa,^[b] and Tatsuya Okubo^{*[a]}

Abstract: The Al location in zeolites can have massive influences on the zeolite properties because it directly correlates with cationic active sites. Here, the synthesis of IFR zeolites with controlled Al distribution at different tetrahedral sites (T sites) is reported. The computational calculations suggest that organic structure-directing agents (OSDAs) used for zeolite synthesis can alter the energetically favorable T sites for Al. Zeolite products synthesized under an identical condition but with different OSDAs are found to have altered fractions of Al at different T sites in accordance with the energies derived from the zeolite–OSDA complexes. Our finding thus provides evidence for the ability of OSDAs to direct Al into more energetically favorable T sites, thereby offering rationally synthetic guidelines for the selective placement of Al into specific crystallographic sites.

Zeolite, an important class of microporous crystalline materials with precisely defined pores and cavities, has been practically used in several industries.^[1] Its structure is built by infinite connection of $TO_{4/2}$ tetrahedra (T is tetrahedral atoms such as Si and Al). Control of local structures of zeolites is of great scientific and technological importance because only small changes at an atomic scale can have significant influences on properties and performance of zeolites. In particular, the location of Al directly correlates with the location of cationic active species because trivalent Al in the silicate zeolite frameworks creates negative charges that require cationic counterions for charge compensation.^[2]

If the counterion is a proton, zeolites can express Brønsted acidity. The acid activity is known to be dependent on the location of Al–O–H since the deprotonation of protons can be influenced by slight changes in atomic environments, and the protons must be in the appropriate locations for efficient interactions with reactants and transient intermediates.^[3] The location of Al is also vital for the transition metal-exchanged zeolites that act as efficient catalysts for selective catalytic reduction of NO_x and partial oxidation of methane because the amount and location of Al determine the nature of active bare multivalent cations or metal-oxo species.^[4]

Because of such significant influences, the community has developed characterization techniques to quantify the Al distribution^[5] and established the synthetic method to control the Al location.^[3c,6,7] Early studies compared the distribution of Al in commercial zeolites and in zeolites synthesized with substantially different protocols.^[6] However, it is impossible to explicitly attribute the differences in the Al locations to the respective synthetic conditions. Later, several studies attempted to minimize the effects caused by the complicatedly interrelated, synthetic parameters;^[3c,7] nevertheless, the relationship between the Al locations and the synthetic parameters is still unclear. The rational design of synthetic parameters to selectively place Al into the desired site remains elusive.

Recently, our group computationally investigated more than 43,000 representative zeolite models having different framework structures, chemical compositions, and Al locations.^[8] Throughout the analyses, we found that the energetically favorable Al locations predicted by computations can well explain experimentally observed Al locations in zeolites synthesized by some specific routes,^[9] suggesting that zeolites with specific Al locations can be attained as an “equilibrium” product by controlling the energetic pathways of crystallization to achieve (on average) more energetically favorable atomic configurations.^[8,9b] These findings have motivated us to rationally design the location of Al in zeolites by controlling the energy difference. Among many possible synthetic parameters, we have selected organic structure-directing agents (OSDAs) for a proof-of-concept. When bulky and water-soluble organic cations are used as OSDAs, they can often direct the crystallization of specific zeolite frameworks having cavities commensurate with their molecular structures.^[10] In addition, OSDAs can control the chemical composition of zeolites by charge compensation, implying that the organic cations strongly interact with negative charges induced by Al. A recent study took these advantages by using OSDAs structurally similar to transition states of targeted catalytic reactions to create effective confinement volumes and active sites in zeolite catalysts.^[11] These intuitive concepts rationalize the approach to regulate the location of Al by employing appropriate OSDAs.

Herein, we demonstrate that the occupancy of Al at different crystallographic T sites of zeolites can be tuned by OSDAs. Three different OSDAs shown in Figure 1a are used to crystallize aluminosilicate zeolites with IFR topology, also known as ITQ-4, SSZ-42, and MCM-58,^[12] under an identical condition. The one-dimensional pore of IFR zeolite is composed of the sequence of cavities that tightly accommodate OSDAs on a one-by-one manner (Figure 1b). This unique structural matching makes IFR zeolite an ideal model for investigation of the Al site-directing ability of OSDAs because it is expected to minimize the mobility of OSDAs.

[a] K. Muraoka, Prof. W. Chaikittisilp, Prof. T. Okubo, Department of Chemical System Engineering The University of Tokyo 7-3-1 Hongo, Bunkyo-ku, Tokyo 113-8656 (Japan) E-mail: watcha@chemsys.t.u-tokyo.ac.jp okubo@chemsys.t.u-tokyo.ac.jp

[b] Y. Yanaba, Prof. T. Yoshikawa Institute of Industrial Science The University of Tokyo 4-6-1 Komaba, Meguro-ku, Tokyo 153-8505 (Japan)

Supporting information for this article is given via a link at the end of the document.

COMMUNICATION

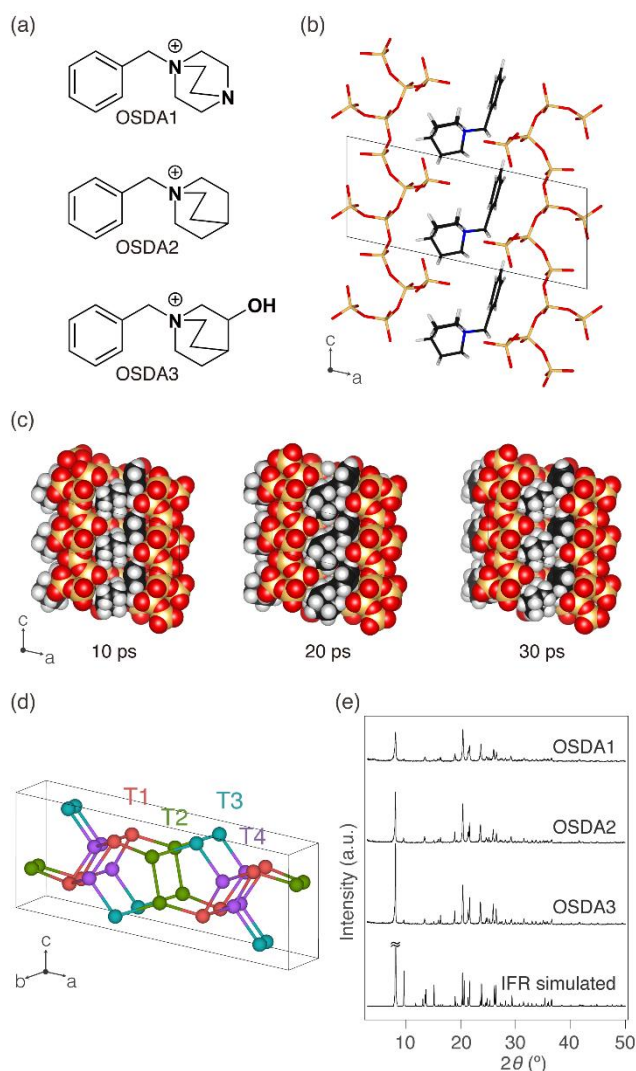


Figure 1. (a) Chemical structures of three OSDAs. (b) Schematic of the structural matching between IFR zeolite and OSDA2. Si, O, C, H, and N atoms are visualized as yellow, red, black, white, and blue sticks, respectively. (c) Snapshots of MD run of IFR zeolite and OSDA2. Atoms are visualized as spheres with the same colors in (b) having their corresponding van der Waals radii. (d) Crystal structure of IFR zeolite. O atoms were omitted for clarity. (e) Powder XRD patterns of the products obtained using different OSDAs by two-step heating.

To verify that the structural matching is maintained under the temperature for zeolite synthesis, we performed molecular dynamics (MD) simulations at 443 K. In general, OSDAs are not strictly located in a defined location but move and rotate inside the cavities of zeolites due to thermal energy.^[13] As depicted in the MD snapshots (Figure 1c), nevertheless, the structural matching did not allow for the free movement and rotation of OSDAs, providing the chance of OSDAs to control the Al locations. Another structural reason for selecting IFR zeolite is that its crystal structure has four distinct crystallographic T sites (Figure 1d), making quantitative determination of Al occupancy possible by the ²⁷Al MQMAS NMR technique^[2a,6b] as this technique is not able

to distinguish Al sites in zeolite structures containing too many T sites such as *BEA and MFI zeolites.^[5b,7b]

To minimize any possible effects caused by synthetic factors other than OSDAs, we made intensive attempts to find an identical synthesis condition for IFR zeolite using different OSDAs. Some of our trials are summarized in Table S1 with the corresponding powder XRD patterns shown in Figures S1–S5 in the Supporting Information. The results indicated a trade-off between the stability of OSDA1 at higher temperature and the slow crystallization with OSDA2 and OSDA3 at lower temperature. Consequently, we decided to employ a two-stage heating method for zeolite synthesis. At lower temperature, the organic–inorganic composite is formed where OSDAs become more stable with surrounding inorganic species, thereby avoiding the degradation of OSDAs, while subsequent heating at higher temperature can promote the zeolite crystallization. This approach was effective here especially when the reaction mixture was first treated at 150 °C for 7 days followed by heating at 170 °C for 7 days. For all OSDAs, IFR zeolites were successfully synthesized under exactly the same condition (Figure 1e).

¹³C CP/MAS NMR spectra of the as-synthesized zeolites matched well with their corresponding OSDAs (Supporting Information, Figure S6), suggesting that the OSDAs are stable under this synthesis condition and occluded intact in the as-synthesized products. The contents of OSDAs in IFR zeolites were two OSDAs per unit cell (Supporting Information, Table S2), corresponding to one OSDA per cage, which is in agreement with the MD simulation (Figure 1c). The concentrations of Al in the products were, however, lower than the contents of OSDAs, suggesting that some of OSDAs are charge-balanced by silanol defects typically observed in high-silica zeolites synthesized with OSDAs.^[14] In this study, such a high-silica composition is preferable because the number of Al–O–Si–O–Al species causing unsystematic shift of ²⁷Al MAS NMR^[15] can be minimized with increasing Si/Al ratios. ²⁹Si MAS NMR spectra (Supporting Information, Figure S7) confirmed that the Al–O–Si–O–Al species were hardly observed (i.e., the absence of signal arising from the Q⁴(2Al) (Si/(AlO)₂(SiO)₂) silicon species). The presence of Q⁴(0Al) (i.e., (Si(SiO)₄) and Q⁴(1Al) (i.e., Si(AlO)(SiO)₃) silicon species corroborated with the crystallization of high-silica zeolites. The peak splitting observed in Q⁴(0Al) signals can be assigned to Si at different crystallographic T sites.^[16]

The IFR samples were analyzed by ²⁷Al 3QMAS NMR to suppress and correctly deal with the quadrupolar effect of ²⁷Al. Several resonances were observed from the obtained spectra (Figures 2a, 2e, and 2i), which can be attributed to the different Al environments. The differences in the two-dimensional spectra suggested the difference in Al environments depending on the OSDAs because other synthesis conditions were identical. The projection of the 3QMAS NMR spectra toward F1 direction (Figures 2b, 2f, and 2j), which is free from quadrupolar broadening, highlighted the differences between samples. The differences were also observed from the projection toward F2 direction affecting the broadening of the signals (Figures 2c, 2g, and 2k). The deconvolution of the spectra using four Voigt functions successfully simulated the experimental projection spectra. Note

COMMUNICATION

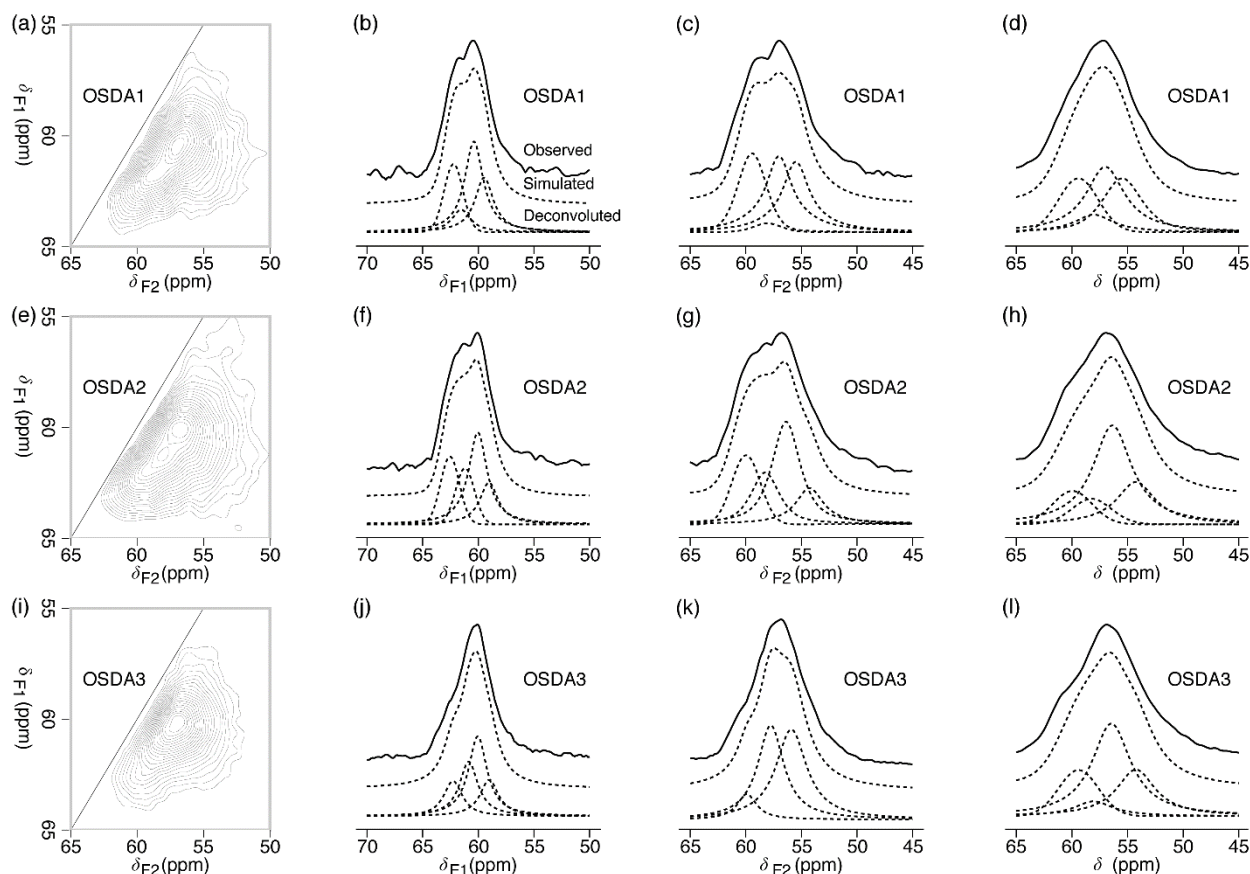


Figure 2. ^{27}Al NMR spectra of IFR zeolites synthesized with (a–d) OSDA1, (e–h) OSDA2, and (i–l) OSDA3. (a, e, i) Two-dimensional plots of 3QMAS NMR spectra with their projections to (b, f, j) F1 and (c, g, k) F2 axes, and (d, h, l) their corresponding single-pulse NMR spectra. Dash lines show simulated spectra deconvoluted using Voigt functions.

that the width of the peaks was fixed^[5b,17] for the same projections. These four resonances presumably corresponded to the different Al locations at four T sites in IFR zeolite. The isotropic chemical shifts were then computed from the chemical shifts in F1 and F2 projections.^[5b,6b]

The computed isotropic chemical shifts can be compared with the theoretical values obtained from the electronic structure calculation using DFT. To calculate the theoretical isotropic chemical shifts, we performed structure optimization of aluminosilicate IFR zeolites with OSDAs. Subsequently, cluster models were extracted from the final optimized structure to compute NMR parameters using a Gauge-Independent Atomic Orbital (GIAO) method.^[18] The theoretically predicted isotropic chemical shifts were in a range of 57–62 ppm, agreed remarkably well with the experimental values (Supporting Information, Table S3). The strong correlation between theoretical and experimental isotropic chemical shifts was observed for all OSDAs (Supporting Information, Figure S8), thereby justifying the techniques used here. The order of chemical shifts was $T3 > T4 > T1 > T2$ for OSDA1 and OSDA2, while the order of OSDA3 was $T4 > T3 > T1 > T2$. This kind of reordering of chemical shifts depending on the types of counter-cations was also observed previously.^[19]

Quantitative estimation of the amount of Al in each T site was obtained from single-pulse ^{27}Al MAS NMR. The absence of the chemical shift arising from the octahedral coordination of Al (at ca. 0 ppm), confirmed that all Al atoms were in the zeolite samples as tetrahedrally coordinated species (Supporting Information, Figure S9). Although the spectra were broadened due to the quadrupolar effect of ^{27}Al , the differences among spectra due to the different OSDAs were apparent, particularly at a shoulder around 61 ppm (Figures 2d, 2h, and 2l). These differences can explicitly be visualized by deconvolution using the simulated spectra in the processing for δ_{F2} . Four Voigt functions with the same width were able to simulate the experimentally observed single-pulse ^{27}Al MAS NMR spectra (Figures 2d, 2h, and 2l).

The observed occupancy varied in a range of 8–54% (Figure 3a), suggesting that there is the bias for the incorporation of Al in IFR zeolites depending on the OSDAs used and the T sites. Note that IFR framework structure has 4 equally weighted T sites, which can imply that if Al is randomly distributed in zeolite, the occupancy of Al should be equally for each T site (i.e., 25%). The most Al-rich site for all OSDAs was T1 with the occupancy of 39–54%, suggesting the intrinsic preference of T1 for Al in the combinations of IFR framework and three OSDAs. The lowest occupancy of 8% was observed for T3 with OSDA3.

COMMUNICATION

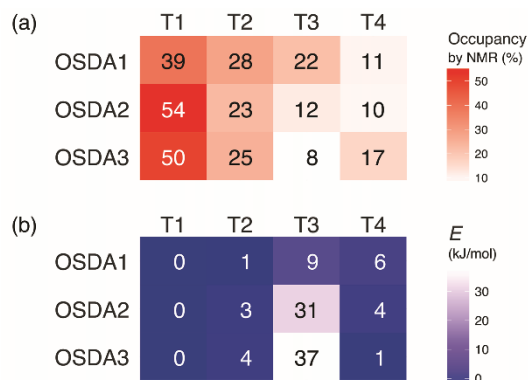


Figure 3. (a) Heatmap of Al occupancy found in IFR zeolites synthesized using different OSDAs. (b) Heatmap of relative energies of aluminosilicate IFR zeolites having Al at different T sites with three OSDAs.

To explain the origin of the differences in the occupancy of Al, we retrieved the bulk energies obtained from the structure optimization using the electronic structure calculation. For each combination of OSDAs and T sites, the lowest energy was computed. As shown in Figure 3b, T1 was the most stabilized crystallographic location for Al, regardless the types of OSDAs, which is clearly matched with the highest occupancy of T1 observed by NMR. Their energies were used as the standard (i.e., 0 kJ/mol) for other T sites. The two closest $N^+ \cdots O(Al)$ distances observed for OSDA1 and T1 were 4.35 and 4.57 Å (Figure 4a). The values for OSDA2 and T1 were essentially identical (Figure 4c). The distances slightly changed but were similar values for OSDA3 (Figure 4e). The close distances of $N^+ \cdots O(Al)$ seemed to stabilize the IFR–OSDA complex and hence enrich T1 with Al.

In contrast, the computed energies of T3 were highest among T sites for all OSDAs. In particular, the combination of T3 and OSDA3 created the least stable electronic structure (37 kJ/mol), consistent with the lowest occupancy of 8% estimated from the NMR spectrum. These results were again in agreement with the $N^+ \cdots O(Al)$ distances (Figure 4f). The two closest distances between OSDA3 and O(Al) for T3 were 6.21 and 6.46 Å, about 2 Å longer than those of T1, seemingly destabilized the system. This tendency is also observed for OSDA2 and O(Al) for T3 (Figure 4d). The occupancy of Al at T3 dramatically improved in the case of OSDA1 (i.e., 22%) compared to other OSDAs. This is consistent with its lower relative energy of 9 kJ/mol, in comparison with 31 and 37 kJ/mol for OSDA2 and OSDA3, respectively. In spite of these dramatic changes in energy, the $N^+ \cdots O(Al)$ distance (6.03 Å) was slightly shorter (Figure 4b), which cannot explain the increasing Al occupancy. The special feature of OSDA1 is that it has another N atom. The distance between this neutral N and the closest O(Al) was 3.70 Å, which can likely enhance the overall stabilization.

In general, the Al distribution in zeolites is thought to be controlled kinetically; however, there exist exceptional cases where the energetic stability is considered to be a dominant determining factor.^[8,9] In the former case, the formation of zeolite is governed by highly mobile OSDAs.^[5b] As a result, the

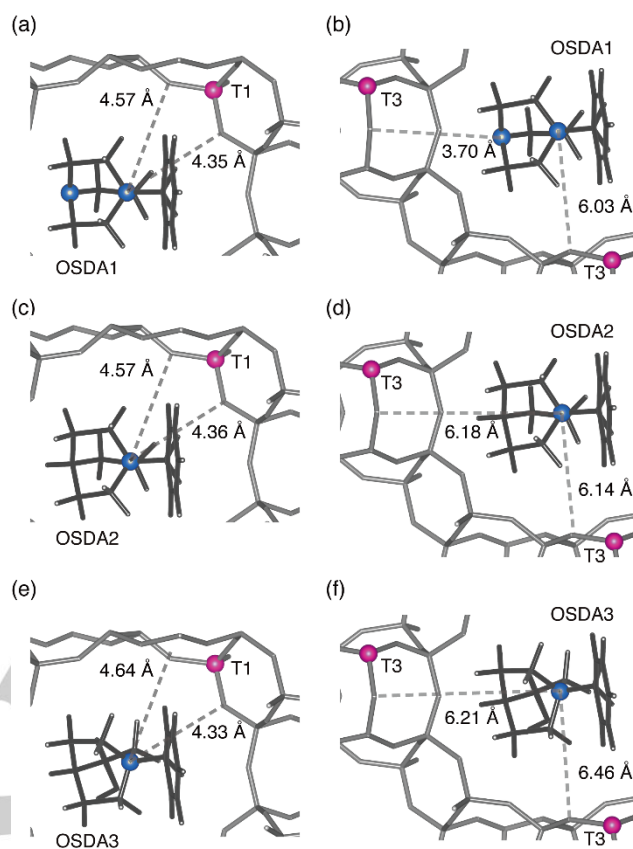


Figure 4. Optimized structures of zeolite–OSDA complexes with (a, b) OSDA1, (c, d) OSDA2, and (e, f) OSDA3 having Al at (a, c, e) T1 and (b, d, f) T3. The pink spheres denote Al, while the blue spheres denote N.

interactions between OSDAs and anionic charges near Al sites are inconstant, leading to broad distributions of Al over T sites. Yet, the Al locations can be controlled in zeolite framework positions between different cavities (e.g., large vs. small cages) but not crystallographic site specific.^[3a,3c,7b] In the latter situation, the T site-specific Al can be achieved due to the low mobility of OSDAs, providing the specificity of the structure-directing ability.^[7a]

The clear correlation between thermodynamic stability of Al at different T sites and Al occupancy described here provides evidence that for IFR zeolites the Al location is primarily governed by the energetic preferences. This phenomenon is likely derived from the tight packing between IFR zeolite and OSDAs, yielding the notable Al site-directing ability of OSDAs. Although a comprehensive understanding why we are able to control such the energetic pathways remains elusive, we surmise that the exceptional matching between zeolite and OSDAs, which can suppress the free movement and rotation of OSDAs, and/or the relatively slow crystallization under the present conditions are essential factors.

In summary, we report that the Al occupancy at different T sites in IFR zeolites synthesized under an identical condition but with different OSDAs can be tuned, in accordance with relative

COMMUNICATION

energies derived from the zeolite–OSDA complexes, suggesting that the Al locations are primarily governed by the energetic preferences to yield (on average) lower energetic atomic configurations. This combined computational and experimental approach provides a paramount step toward the rational synthesis of zeolites with selectively controlled Al locations. It is anticipated that the insight obtained from this model system can be applied to other related framework materials.

Acknowledgements

W. C. thanks JSPS (KAKENHI 16K18284) and the Asahi Glass Foundation for financial support. K. M. has received financial support from JSPS (DC1) and the Program for Leading Graduate Schools, “Global Leader Program for Social Design and Management (GSDM)”, by MEXT. The computational resources were provided by the Supercomputer Center in Institute for Solid State Physics (ISSP) of The University of Tokyo and Research Center for Computational Science at the Institute for Molecular Science (IMS) in Okazaki, Japan.

Keywords: Al siting • Density functional calculations • NMR spectroscopy • Structure-directing agents • Zeolites

- [1] a) M. E. Davis, *Nature* **2002**, *417*, 813–821; b) M. A. Snyder, M. Tsapatsis, *Angew. Chem. Int. Ed.* **2007**, *46*, 7560–7573; *Angew. Chem.* **2007**, *119*, 7704–7717.
- [2] a) J. Dědeček, Z. Sobalík, B. Wichterlová, *Catal. Rev.: Sci. Eng.* **2012**, *54*, 135–223; b) J. Shin, D. S. Bhande, M. A. Cambor, Y. Lee, W. J. Kim, I.-S. Nam, S. B. Hong, *J. Am. Chem. Soc.* **2011**, *133*, 10587–10598.
- [3] a) R. Gounder, E. Iglesia, *Angew. Chem. Int. Ed.* **2010**, *49*, 808–811; *Angew. Chem.* **2010**, *122*, 820–823; b) N. Katada, K. Suzuki, T. Noda, G. Sastre, M. Niwa, *J. Phys. Chem. C* **2009**, *113*, 19208–19217; c) Y. Román-Leshkov, M. Moliner, M. E. Davis, *J. Phys. Chem. C* **2011**, *115*, 1096–1102.
- [4] a) C. Paolucci, I. Khurana, A. A. Parekh, S. Li, A. J. Shih, H. Li, J. R. Di Iorio, J. D. Albarracin-Caballero, A. Yezerets, J. T. Miller, W. N. Delgass, F. H. Ribeiro, W. F. Schneider, R. Gounder, *Science* **2017**, *357*, 898–903; b) S. Grundner, M. A. C. Markovits, G. Li, M. Tromp, E. A. Pidko, E. J. M. Hensen, A. Jentys, M. Sanchez-Sanchez, J. A. Lercher, *Nat. Commun.* **2015**, *6*, 7546.
- [5] a) S. Sklenak, J. Dědeček, C. Li, B. Wichterlová, V. Gábová, M. Sierka, J. Sauer, *Angew. Chem. Int. Ed.* **2007**, *46*, 7286–7289; *Angew. Chem.* **2007**, *119*, 7424–7427; b) A. Vjunov, J. L. Fulton, T. Huthwelker, S. Pin, D. Mei, G. K. Schenter, N. Govind, D. M. Camaioni, J. Z. Hu, J. A. Lercher, *J. Am. Chem. Soc.* **2014**, *136*, 8296–8306; c) H. Koller, T. Uesbeck, M. R. Hansen, M. Hunger, *J. Phys. Chem. C* **2017**, *121*, 25930–25940.
- [6] a) O. H. Han, C.-S. Kim, S. B. Hong, *Angew. Chem. Int. Ed.* **2002**, *41*, 469–472; *Angew. Chem.* **2002**, *114*, 487–490; b) J. Dedecek, M. J. Lucero, C. Li, F. Gao, P. Klein, M. Urbanova, Z. Tvaruzkova, P. Sazama, S. Sklenak, *J. Phys. Chem. C* **2011**, *115*, 11056–11064.
- [7] a) A. B. Pinar, L. Gómez-Hortigüela, L. B. McCusker, J. Pérez-Pariente, *Chem. Mater.* **2013**, *25*, 3654–3661; b) T. Yokoi, H. Mochizuki, S. Namba, J. N. Kondo, T. Tatsumi, *J. Phys. Chem. C* **2015**, *119*, 15303–15315; c) J. R. Di Iorio, R. Gounder, *Chem. Mater.* **2016**, *28*, 2236–2247.
- [8] K. Muraoka, W. Chaikittisilp, T. Okubo, *J. Am. Chem. Soc.* **2016**, *138*, 6184–6193.
- [9] a) M. Ogura, K. Itabashi, J. Dedecek, T. Onkawa, Y. Shimada, K. Kawakami, K. Onodera, S. Nakamura, T. Okubo, *J. Catal.* **2014**, *315*, 1–5; b) M. D. Oleksiak, K. Muraoka, M.-F. Hsieh, M. T. Conato, A. Shimojima, T. Okubo, W. Chaikittisilp, J. D. Rimer, *Angew. Chem. Int. Ed.* **2017**, *56*, 13366–13371; *Angew. Chem.* **2017**, *129*, 13551–13556.
- [10] a) R. F. Lobo, S. I. Zones, M. E. Davis, *J. Inclusion Phenom. Mol. Recognit. Chem.* **1995**, *21*, 47–78; b) M. Moliner, F. Rey, A. Corma, *Angew. Chem. Int. Ed.* **2013**, *52*, 13880–13889; *Angew. Chem.* **2013**, *125*, 14124–14134.
- [11] E. M. Gallego, M. T. Portilla, C. Paris, A. León-Escamilla, M. Boronat, M. Moliner, A. Corma, *Science* **2017**, *355*, 1051–1054.
- [12] a) M. A. Cambor, A. Corma, L. A. Villaescusa, *Chem. Commun.* **1997**, 749–750; b) C.-Y. Chen, L. W. Finger, R. C. Medrud, C. L. Kibby, P. A. Crozier, I. Y. Chan, T. V. Harris, L. W. Beck, S. I. Zones, *Chem. Eur. J.* **1998**, *4*, 1312–1323; c) B. Gil, G. Košová, J. Čejka, *Microporous Mesoporous Mater.* **2010**, *129*, 256–266.
- [13] M. E. Davis, R. F. Lobo, *Chem. Mater.* **1992**, *4*, 756–768.
- [14] G. Bruncklaus, H. Koller, S. I. Zones, *Angew. Chem. Int. Ed.* **2016**, *55*, 14459–14463; *Angew. Chem.* **2016**, *128*, 14675–14679.
- [15] J. Dědeček, S. Sklenak, C. Li, F. Gao, J. Brus, Q. Zhu, T. Tatsumi, *J. Phys. Chem. C* **2009**, *113*, 14454–14466.
- [16] D. H. Brouwer, I. L. Moudrakovski, R. J. Darton, R. E. Morris, *Magn. Reson. Chem.* **2010**, *48*, S113–S121.
- [17] P. Sarv, C. Fernandez, J.-P. Amoureux, K. Keskinen, *J. Phys. Chem.* **1996**, *100*, 19223–19226.
- [18] K. Wolinski, J. F. Hinton, P. Pulay, *J. Am. Chem. Soc.* **1990**, *112*, 8251–8260.
- [19] J. Kučera, P. Nachtigall, *Microporous Mesoporous Mater.* **2005**, *85*, 279–283.

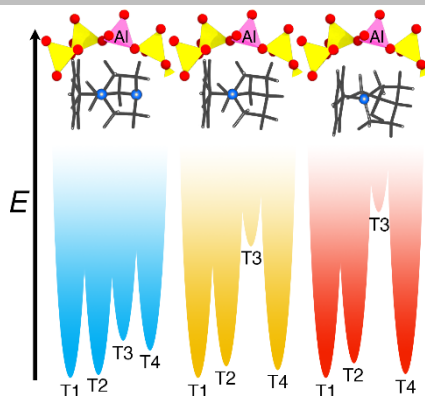
COMMUNICATION

Entry for the Table of Contents (Please choose one layout)

Layout 1:

COMMUNICATION

Put in places: IFR-type zeolites with tuned Al locations at different tetrahedral sites are synthesized with difference organic structure-directing agents (OSDAs), revealing the Al site-directing ability of OSDAs. The occupancy of Al at each site is strongly correlated with the energies of the zeolite–OSDA complexes, suggesting that the Al locations are primarily governed by the energetic preferences.



K. Muraoka, W. Chaikittisilp,*
Y. Yanaba, T. Yoshikawa, T. Okubo*

Page No. – Page No.

Directing Aluminum Atoms into
Energetically Favorable Tetrahedral
Sites in Zeolite Framework by
Organic Structure-Directing Agents